A simple and cost-effective synthesis of ionic porous organic polymers with excellent porosity for high iodine capture

Zhongping Li,[a†*] He Li,[b†] Dongjin Wang,[a†] Athchaya Suwansoontorn,[a] Gang Du,[a] Zhaohan Liu,[a] Md. Mahmudul Hasan,[a] and Yuki Nagao[a*]

[a] School of Materials Science, Japan Advanced Institute of Science and Technology, Japan.

[b] State Key Laboratory of Catalysis, iChEM, Dalian Institute of Chemical Physics, Chinese Academy of Sciences, China.

[c] College of Chemistry, Jilin Normal University, Changchun, 130103, Republic of China.

[†]Z. Li, H. Li, and D. Wang contributed equally.

[*]Corresponding author. E-mail address: lizhongping2013@163.com; ynagao@jaist.ac.jp.

Highlights

- The i-POPs have been synthesized via a simple and cost-effective process.
- The i-POPs showed the highest BET surface area and pore volume.
- The i-POPs exhibited the best iodine uptake value among all reported ionic POPs.
- The capture process could be efficiently recycled and reused for five cycles.

Abstract

Porous organic polymers (POPs) are excellent adsorbent candidates owing to their high porosity, permanent pore, and well-designed structure. Ionic porous organic polymers (i-POPs) are a special type of POPs, which can greatly improve the capacity of guest molecules through electrostatic interactions. However, most reported i-POPs have shortcomings such as low porosity and high-cost synthesis procedure. With these considerations in mind, several ionic porous organic polymers (i-POP-BP-BPTMs) have been successfully designed and synthesized by using the commercial and simple-synthesized building units via a simple and cost-effective process. i-POP-BP-BPTMs indicated excellent porosity including the highest BET surface area (1491-1753 $m^2 g^{-1}$) and the best pore volume (2.19-2.94 $cm^3 g^{-1}$) among most reported ionic POPs. Interestingly, i-POP-BP-BPTM was found to be highly effective in iodine vapor capture up to 415 wt%, which is higher than the value of all reported ionic POPs. These results offer a new way to design and construct functional ionic POPs.

Keywords: Ionic porous organic polymers, facile and low-cost synthesis, high porosity, effective iodine uptake.

Introduction

In recent years, many urgent attentions have been paid to environmental risks, especially nuclear accidents and waste, which stems from widespread use of nuclear energy. Due to the health effects of radiation, the main safety issue associated with nuclear energy is proper nuclear waste management.[1] ^{127}I and ^{129}I are important radioisotope in nuclear waste, especially long-lived half-life (1.57×10^7 years), which has generated great concern. Standard methods for iodine capture focus on inorganic solid adsorbents such as silver-based zeolites.[2] However, these absorbents usually show low capacities, which derive from their limited accessible surface areas. Considering these detrimental effects, designing effective materials for radioactive iodine capture is urgent and essential.

Porous organic polymers (POPs) are a new class of porous polymers that possess high porosity and permanent pore topology/structure. POPs have grown into a thriving family, including conjugated microporous polymers (CMPs),[3-4] polymers of intrinsic microporous (PIMs),[5] covalent organic frameworks (COFs),[6-8] porous aromatic frameworks (PAFs),[9] and hypercrosslinked polymers (HCPs).[10-12] Due to their strong organic bonds linked nature, POPs usually have good thermal/chemical stability. Therefore, POPs have shown potential applications in gas storage, molecular sensing, and catalysis, and pollutants removal.[13-37]

We are interested in porous hyper-crosslinked polymers because they not only possess permanent porosity and remarked stability, but also have the advantages to introduce various functional units by simple and cost-effective synthesis, which can improve guest molecules capture ability.[10] Recently, POPs built-in ionic groups exhibited stronger electrostatic forces towards specific molecules than neutral polymers.[33, 38] However, elaborate synthesis methods and complex organic compounds are required to introduce ionic units into the porous structure, which limited porosity and structure diversity.[38] There is a strong demand to develop ionic porous materials with high porosity by a sample and lower-cost way. In this context, we synthesized neutral porous polymer (POP-BP) that is constructed through commercial raw materials, 4,4'-bis(chloromethyl)-

1,1'-biphenyl (BP), as a crosslinking agent and building unit under solvothermal conditions by cheap $FeCl_3$ as the catalyst via a facile Friedel–Crafts alkylation reaction (Scheme 1a). Then, ionic building unit, 1,1'-([1,1'-biphenyl]-4,4'-diyl)bis(N,N,N-trimethylmethanaminium) chloride (BPTM) easily prepared from BP via one step in a large-scale synthesis, was introduced into the skeleton of POP-BP to afford ionic porous organic polymers (i-POPs). With the increment of ionic unit, the i-POP-BP-BPTM-1, i-POP-BP-BPTM-2, and i-POP-BP-BPTM-3 were successfully synthesized under the same condition (Scheme 1b).

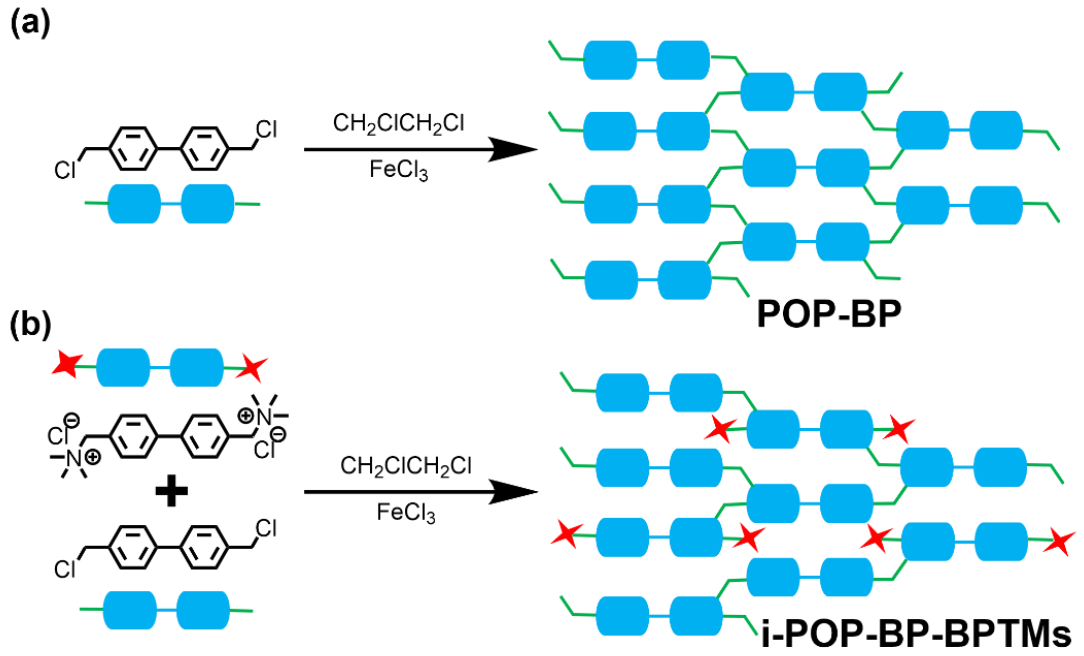

Scheme 1 (a) Schematic representation of the synthesis of (a) POP-BP and (b) i-POP-BP-BPTMs.

Results and discussion

POP-BP was prepared according to a previous report with a high yield of 99%.[11] The construction of ionic polymers was achieved by using BPTM as the monomer, 4,4'-bis(chloromethyl)-1,1'-biphenyl as the crosslinking agent, in the presence of $FeCl_3$ as a catalyst. The component of the polymer was tuned by the variation of the number of monomers, and the resultant polymers were denoted as i-POP-BP-BPTMs (For detail, see experimental section). C, N and H elemental analysis was investigated for the POPs. With the increment of BPTM, the amount of N element was an obvious improvement of networks

(Tab. S1). Among the POPs, i-POP-BP-BPTM-3 showed the highest N content of 2.87%. The successful crosslinking of i-POP-BP-BPTMs was confirmed by FT IR measurements. The obvious peaks at 2916-3021 cm^{-1} could be attributed to the C-H stretching vibration, which originated from the structure of $–CH_2–$ and $–CH_3$ in the frameworks (Fig. 1). The C-N bond vibration was observed at 1219 cm^{-1} of i-POP-BP-BPTMs, which is the same as that of BPTM. In the ^{13}C NMR spectrum of i-POP-BP-BPTM-3, the signals at 128 and 139 ppm were assigned to aromatic carbon (Fig. S1). There were obvious peaks at 37.1 and 53.0 ppm for $-CH_2-$ and $-CH_3-$ of i-POP-BP-BPTM-3.

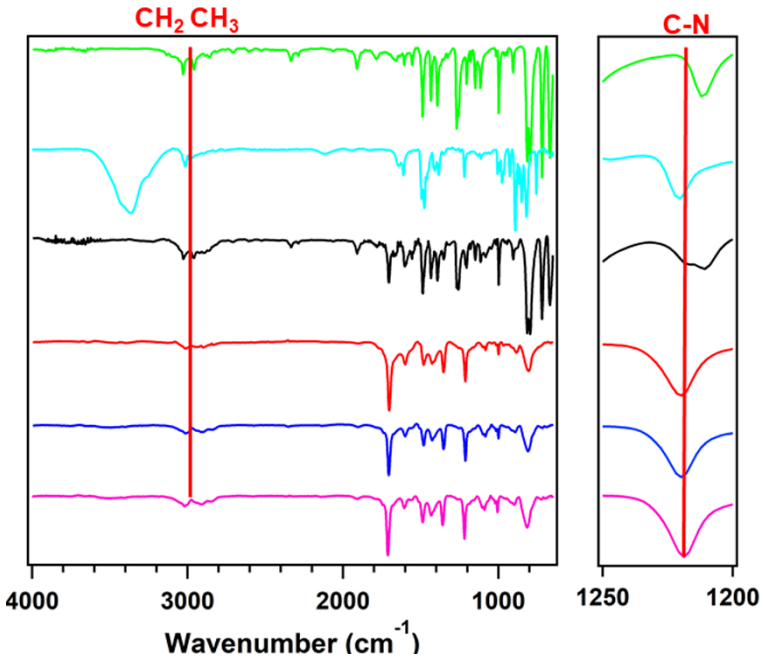

Fig. 1. FT IR spectra of BP (green curve), BPTM (sky-blue), POP-BP (black curve), i-POP-BPTM-1 (red curve), i-POP-BP-BPTM-2 (blue curve), and i-POP-BPTM-3 (purple curve).

Scanning electron microscopy (SEM) images were conducted to investigate the morphology of the materials, and all the POPs exhibited morphology as aggregated micrometer-scale particles (Fig. S2). The elemental mapping by energy-dispersive X-ray spectroscopy (EDS) analysis result of i-POP-BP-BPTMs also proved the existence of N and Cl elements (Fig. S3). Interestingly, EDS mapping result of i-POP-BP-BPTMs indicated a relatively uniform distribution of N and Cl in networks. The thermal stability of the

polymers was investigated by thermogravimetric analysis (TGA) under a nitrogen atmosphere (Fig. S4). Among these polymers, POP-BP has good thermal ability, which could be stable up to 350 °C. For i-POP-BP-BPTMs, as the increasement of BPTM in the polymer, the decomposition temperature decreased. Powder X-ray diffraction measurements (PXRD) of POPs suggested their amorphous structures (Fig. S5).

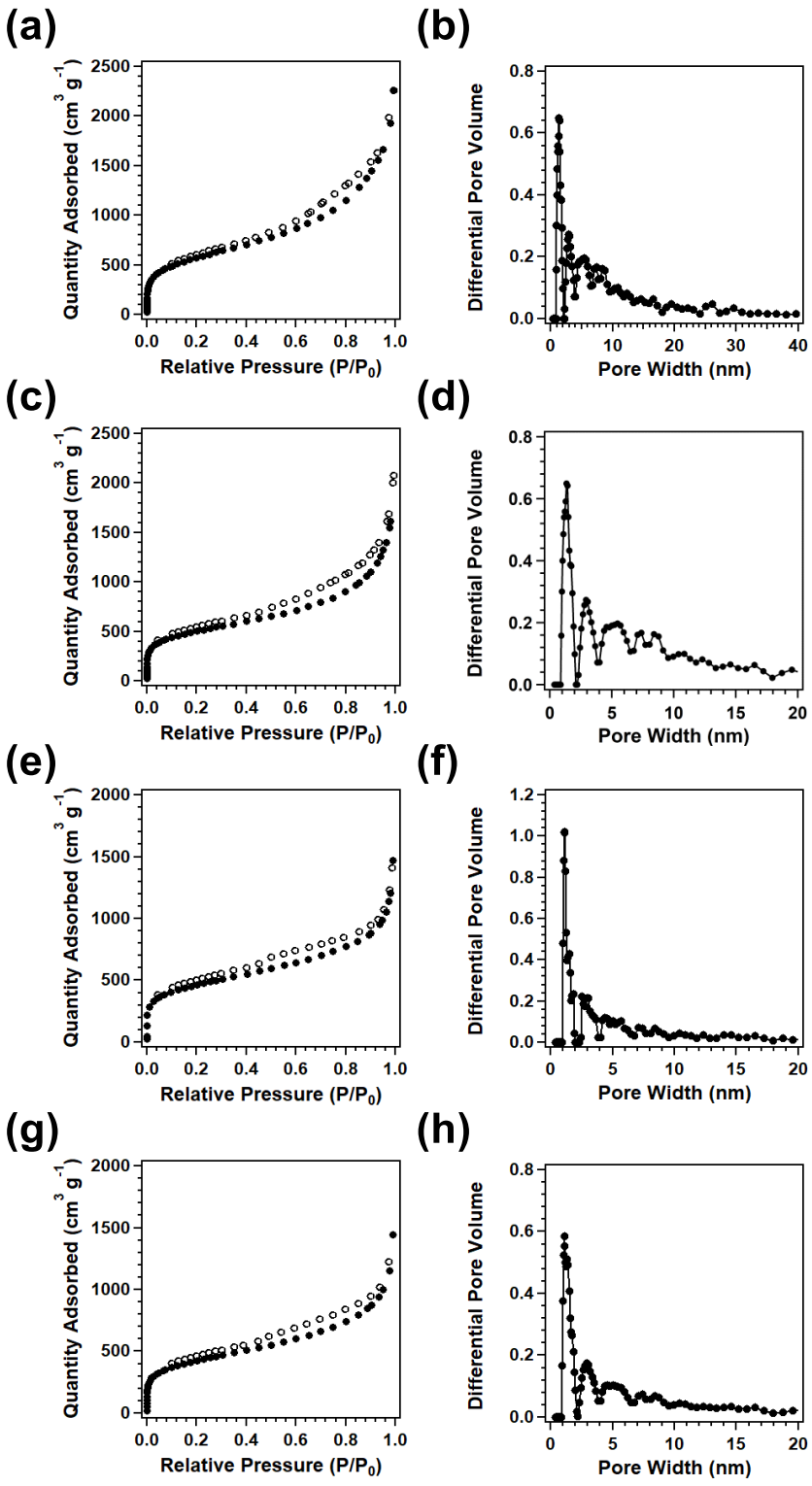

Fig. 2. Nitrogen sorption isotherms of (a) POP-BP, (c) i-POP-BP-BPTM-1, (e) i-POP-BP-BPTM-2, and (g) i-POP-BP-BPTM-3 measured at 77 K (●: adsorption, ○: desorption). Pore size distribution of (b) i-POP-BP, (d) i-POP-BP-BPTM-1, (f) i-POP-BP-BPTM-2, and (h) i-POP-BP-BPTM-3.

Table I. Porosity of POPs

Name	BET surface Area ($m^2\ g^{-1}$) [a]	Pore Volume ($cm^3\ g^{-1}$) [b]	Pore Size (nm) [c]
POP-BP	2039	3.38	1.40, 2.93, 5.47
i-POP-BP-BPTM-1	1753	2.94	1.36, 2.93, 5.46
i-POP-BP-BPTM-2	1611	2.44	1.12, 2.92, 4.56
i-POP-BP-BPTM-3	1491	2.19	1.09, 2.91, 4.50

[a] The BET surface area was calculated through the nitrogen adsorption isotherms by using the BET method. [b] Total pore volume was estimated at a P/P_0 of 0.99. [c] The pore size was calculated from nonlocal density functional theory (NLDFT).

The permanent porosities of POPs were investigated by nitrogen adsorption measurements at 77 K. As shown in Fig. 2, All the prepared POPs showed type I isotherm with sharp uptake observed in the low pressure, which is a representative character of microporosity according to the IUPAC classification. POP-BP showed the highest Brunauer–Emmett–Teller (BET) surface area of 2040 $m^2\ g^{-1}$ with the pore volume of 3.38 $cm^3\ g^{-1}$. Introducing ionic building blocks into the network also gave high porosity for ionic polymers. i-POP-BPTM-1, i-POP-BPTM-2, and i-POP-BP-BPTM-3 displayed high BET surface area of 1753, 1611 and 1485 $m^2\ g^{-1}$, respectively. To our best knowledge, the BET surface area of i-POP-BPTMs is higher than that of all reported ionic POPs (Table S2).[21, 26, 38-48] The i-POP-BPTM-1, i-POP-BPTM-2, and i-POP-BPTM-3 displayed remarkable pore volume of 2.95, 2.24, and 2.19 $cm^3\ g^{-1}$, respectively, which was also higher than the most reported ionic POPs. The excellent porosity of i-POP-BP-BPTMs is possibly due to its high polymerization degree and reactivity of 4,4'-bis(chloromethyl)-1,1'-biphenyl. The pore size distribution of POPs was evaluated using nonlocal density functional theory (NLDFT). POP-BP exhibited a wide pore size distribution from 1.40, 2.93, to 5.47 nm, and the main pore size of POP-BP is at 1.40 nm, which proved its microporous nature. Due to the introduction of a larger building unit of BPTM into the polymer network, the pore was

partially blocked, and the main pore size was centered at 1.09 to 1.36 nm for i-POP-BP-BPTMs.

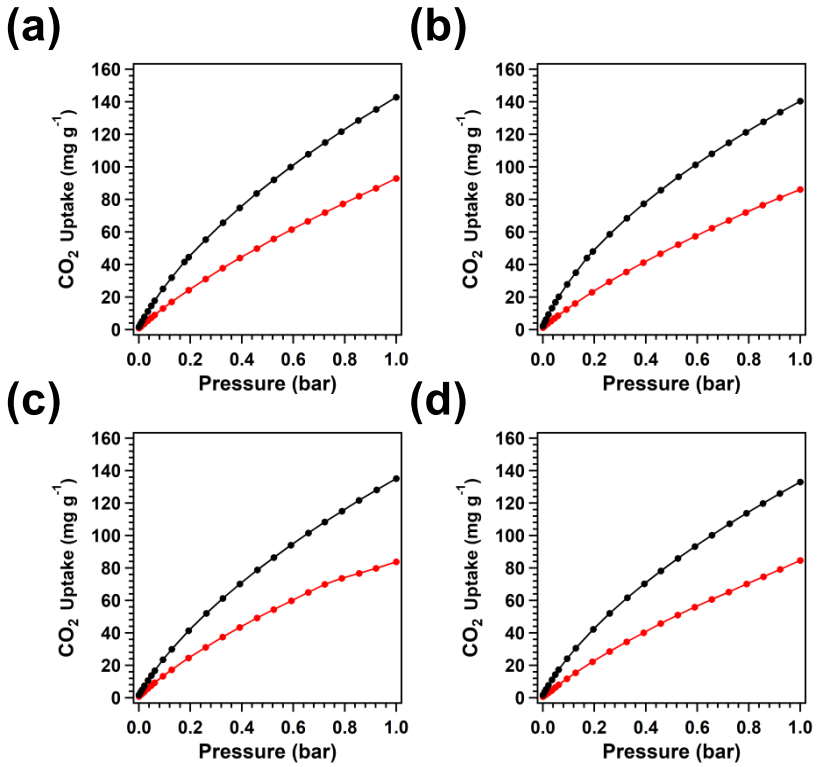

Fig. 3. Carbon dioxide capture of (a) POP-BP, (b) i-POP-BP-BPTM-1, (c) i-POP-BP-BPTM-2, and (d) i-POP-BP-BPTM-3 measured at 298 K (red curve) and 273 K (black curve) under 1.0 bar.

The carbon dioxide uptake properties of the POPs were investigated at 298 K and 273 K (Fig. 3). The carbon dioxide isotherms of POP-BP showed a carbon dioxide uptake of 143 mg g^{-1} at 273 K and 1 bar. At the same condition, i-POP-BP-BPTM-1, i-POP-BP-BPTM-2, and i-POP-BP-BPTM-3 displayed carbon dioxide uptake of 140, 136, and 131 mg g^{-1} at 273 K and 1 bar, respectively. With the increment of ionic units in the skeleton, the carbon dioxide capture ability of i-POP-BPTMs decreased. This is because the ionic units blocked the pores and reduced porosity. The isosteric heats of adsorption (Qst) for carbon dioxide were estimated from the adsorption data collected at 273 K and 298 K. The Qst of i-POPs was calculated to be 20-30 kJ mol^{-1} (Fig. S6). This indicated the physical adsorption nature of CO_2 for all the prepared polymers.

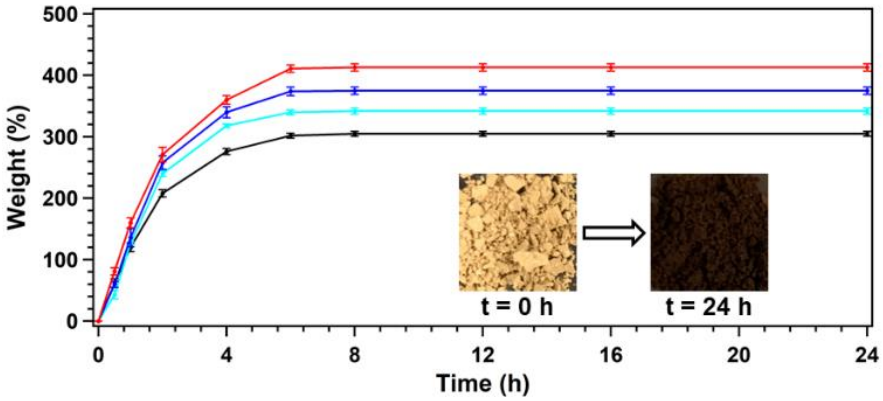

Fig. 4. (a) Iodine vapor capture profiles of the POP-BP (black curve), i-POP-BP-BPTM-1 (sky curve), i-POP-BP-BPTM-2 (blue curve), and i-POP-BP-BPTM-3 (red curve) as a function of exposure time at 350 K and ambient pressure. Inset: the photographs reveal the color change of the samples of i-POP-BP-BPTM-3 before and after iodine adsorption.

Owing to their high BET surface area and pore volume, and abundant ionic sources of i-POP-BP-BPTMs, we investigated the iodine vapor capture property by exposing the i-POP polymers into iodine vapor at 350 K under ambient pressure, which are typical nuclear fuel reprocessing conditions. As time progressed, i-POP samples showed the quick adsorption towards iodine and steep increase within 6 h, and the maximum adsorption capacity of i-POP polymers was reached relatively quickly (Fig. 4). No significant weight gain of the samples was observed after 12 h, which indicated the system was saturated. The neutral POP-BP showed iodine uptake of 305 wt% at 24 h. With increment of ionic units, the maximum adsorption capacity was greatly improved. For example, the saturated iodine loading is up to 342 and 375 wt% for i-POP-BPTM-1 and i-POP-BPTM-2, respectively. Interestingly, i-POP-BPTM-3 showed the highest capture ability of 415 wt%, which is higher than most reported i-POPs (Tab. S3) such as PAF-25 (260 wt%)[44] PAF-24 (276 wt%),[44] COP1^{++} (212 wt%),[45] CalP4-Li (312 wt%),[46] PHF-1-Ct (405 wt%),[47] CTF-Cl-1 (268 wt%).[48] This value is comparable to various neutral POPs [49-66] such as NiP-CMP (202 wt%),[49] TPT-TAPB-COF (251 wt%),[51] Tm-MTDAB (304 wt%),[52] NRPP-2 (222 wt %),[54] NOP-5 (202 wt%),[59] NTP (180 wt%),[61] BDP-CPP-1 (283 wt%),[64] HFCMP (TTPB) (443 wt%).[66]

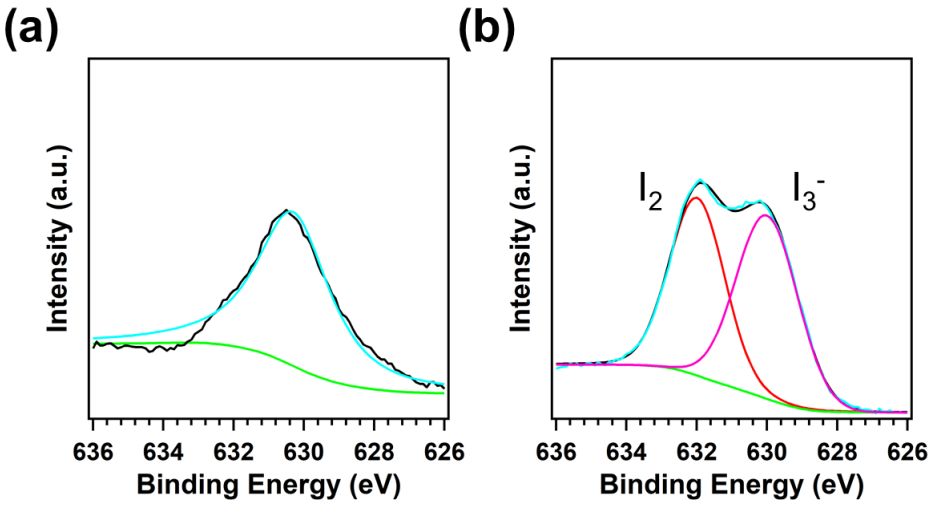

Fig. 5. I 3d XPS spectra of (a) POP-BP@I_2 and (b) i-POP-BPTMs@I_2.

We investigated the mechanism of the iodine capture process by XPS results of POPs. POP-PB@I_2 showed only a valence of zero were detected, which confirmed neutral iodine remained in the network (Fig. 5a). This indicated that a purely physical adsorption process of iodine in POP-BP. Meanwhile, both neutral I_2 and anion I_3^- were observed in i-POP-BPTMs@I_2 complex (Fig. 5b), which indicate that some iodine molecules were transformed into I_3^-. The improvement of iodine capture ability is attributed to ionic units on the walls of networks. Increasing the ionic units of networks may produce electrostatic interactions between the positively charged ionic groups and iodine molecules.[33, 48]

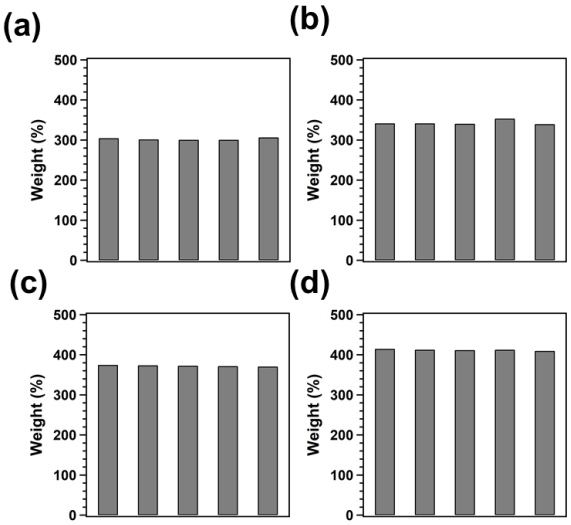

Fig. 6. Cycle performances of iodine capture for (a) POP-BP, (b) i-POP-BPTM-1, (c) i-POP-BPTM-2, and (d) i-POP-BPTM-3.

We investigated the cycle performance for I_2 capture. POPs@I_2 samples were dispersed in ethanol and then filtered and washed by ethanol for several times until no color is in the solution. The regenerated POPs were tested for the next absorption. To our surprise, all networks could be efficiently recycled and reused for five cycles without significant loss of iodine uptake (Fig. 6). FT IR analysis results indicated that POPs remained structure before and after I_2 capture after five cycles (Fig. S7).

Conclusions

Several novel ionic porous organic polymers were successfully designed and constructed by using the commercial and simple-synthesized building units via the Friedel–Crafts alkylation reaction, which is an easy and cost-effective method. The synthesized i-POPs showed high BET surface area (1491-1753 $m^2\ g^{-1}$) and pore volume (2.19-2.94 $cm^3\ g^{-1}$), which is much higher than that of all reported i-POPs. i-POPs improved the iodine capture than neutral material through the electrostatic forces. Importantly, i-POPs also showed high iodine capture ability up to 415 wt% and five cycles of performance without losing ability. We also highlight that this research opens a new way for the construction of ionic porous organic polymers with low-price and simple-synthesis. Currently, the new design and synthesis of functional i-POPs for energy, environment, and catalysis-related fields are underway in our laboratory.

Experimental

Materials and methods

4,4'-Bis(chloromethyl)-1,1'-biphenyl, trimethylamine, iodine, hydrochloric acid, dimethylacetamide, tetrahydrofuran, acetone, methanol, and ethanol were obtained from TCI and Wako. Anhydrous iron (III) chloride and 1,2-dichloroethane were bought from Sigma-Aldrich. ^1H NMR spectra were recorded on a Varian Mercury-500 NMR spectrometer, where chemical shifts (δ in ppm) were determined with a residual proton of

the solvent as standard. Fourier transforms Infrared (FT IR) spectra were recorded from 650 to 4000 cm^{-1} on a Fourier-transform infrared spectrometer (Nicolet 6700; Thermo Fisher Scientific Inc.). Elemental analyses were carried out on a CHNS element analysis VarioEL3. Scanning electron microscope (SEM) was performed on HITACHI Miniscope TM3030. Energy-dispersive X-ray spectroscopy (EDS) mapping was measured by TM3030Plus miniscope. Powder X-ray diffraction (PXRD) data were recorded on fully automatic horizontal multipurpose X-ray diffractometer (Rigaku Smartlab) (Cu Kα, λ = 0.154 nm) by depositing powder on the glass substrate, from 2θ = 1.5° up to 30° with 0.02° increment. Nitrogen sorption isotherms were measured at 77 K by BELSORP-Max. The Brunauer-Emmett-Teller (BET) method was utilized to calculate the specific surface areas. By using the non-local density functional theory (NLDFT) model, the pore volume was derived from the sorption curve.

Synthetic procedures

Synthesis of 1,1'-([1,1'-biphenyl]-4,4'-diyl)bis(N,N,N-trimethylmethanaminium) chloride (BPTM): 4,4'-Bis(chloromethyl)-1,1'-biphenyl (BP) (2.5 g, 0.01 mmol) was dissolved into dimethylacetamide (20 mL) at room temperature. Then, the trimethylamine (5.4 mL, 0.06 mmol) was added into the solution. The system was stirred for 48 hours at room temperature. The mixture was poured into tetrahydrofuran 150 mL, and stirred at 10 mins. The precipitate was collected and washed by THF, and dried under vacuum at room temperature overnight to afford white powder in 93% isolated yield. ^{1}H NMR (400 MHz, D_2O): δ 7.75-7.77 (d, 4H), 7.56-7.58 (d, 4H), 4.45 (s, 4H), 3.03 (s, 18H) ppm.

Synthesis of POP-BP: The POP-BP was synthesized using reported methods.[11] The

bis(chloromethyl)-1,1'-biphenyl (70 mg, 0.28 mmol), anhydrous $FeCl_3$ (91 mg, 0.56 mmol), and 1,2-dichloroethane 4 mL were added the flask. The mixture was stirred for 1 min, degassed through three freeze-pump-thaw cycles, and heated at 80 ºC for 48 h under Ar atmosphere. The precipitate was collected and washed with water and acetone, and soxhleted with methanol for 24 h. The initial polymer was stirred with HCl (1M 20 mL) overnight, filtered and washed by water and acetone, and dried under vacuum at room temperature for 24 hours to afford brown powder in 99% isolated yield.

Synthesis of i-POP-BP-BPTM-1: Bis(chloromethyl)-1,1'-biphenyl (70 mg, 0.28 mmol), 1,1'-([1,1'-biphenyl]-4,4'-diyl)bis(N,N,N-trimethylmethanaminium) chloride (BPTM) (51.5 mg, 0.14 mmol), anhydrous $FeCl_3$ (91 mg, 0.56 mmol) and 1,2-dichloroethane 4 mL were added the flask. The mixture was stirred for 1 min, degassed through three freeze-pump-thaw cycles, and heated at 80 ºC for 48 h under Argon atmosphere. The precipitate was collected and washed with a larger amount of water and acetone, and soxhleted with methanol for 24 hours. The initial polymer was stirred by HCl 1M 20 mL overnight, filtered and washed by water and acetone, and dried under vacuum at room temperature for 24 hours to afford light-brown powder in 78% isolated yield. The synthesis method of i-POP-BP-BPTM-2, and i-POP-BP-BPTM-3 was the same as the i-POP-BP-BPTM-1. The ration of BP and BPTM was 1:1 and 1:3 for i-POP-BP-BPTM-2, and i-POP-BP-BPTM-3, respectively. (There is a larger amount molar ratio of BPTM than reactivity sites of BP to enhance the ionic units for i-POP-BP-BPTM-3).

Iodine vapor sorption

Three open vials (2 mL) with POP samples were placed in a large vial (20 mL) containing

iodine (3 g). This system was sealed and kept in an oven at 350 K. After a period of time, the system was cooled down to room temperature. The small vial containing the POP samples were weighted and placed back into the system. Then, the system was put back in the oven at 350 K to continue the adsorption until the mass of the small vial containing the POP samples did not change. The POPs@I_2 samples were added to EtOH (10 mL) at 2 h. This operation was repeated until the solution showed no color changes. The POP samples were filtered and washed with ethyl alcohol, dried under vacuum at room temperature at 24 h and reused for the next cycle.

Conflicts of interest

There are no conflicts to declare.

Acknowledgements

Z. L. appreciates the support by JSPS KAKENHI grant number JP18J13699. Z. L. also expresses gratitude to Prof. Shun Nishimura, Prof. Noriyoshi Matsumi, and Mr. Xianzhu Zhong for nitrogen adsorption measurement and other experiments.

References

1. G. Mushkacheva, E. Rabinovich, V. Privalov, S. Povolotskaya, V. Shorokhova, S. Sokolova, V. Turdakova, E. Ryzhova, P. Hall, A. B. Schneider, D. L. Preston, E. Ron, Thyroid abnormalities associated with protracted childhood exposure to ^{131}I from atmospheric emissions from the mayak weapons facility in Russia, Radiat. Res.,166 (2006), pp.715–722.

2. K. W. Chapman, P. J. Chupas, T. M. Nenoff, Radioactive iodine capture in silver-containing mordenites through nanoscale silver iodide formation, J. Am. Chem. Soc., 132 (2010), pp.8897–8899.
3. J. X. Jiang, F. B. Su, A. Trewin, C. D. Wood, N. L. Campbell, H. J. Niu, C. Dickinson, A. Y. Ganin, M. J. Rosseinsky, Y. Z. Khimyak, A. I. Cooper, Conjugated microporous poly(aryleneethynylene) networks, Angew. Chem. Int. Ed., 46 (2007), pp. 8574–8578.
4. Y. Xu, S. Jin, H. Xu, A. Nagai, D. Jiang, Conjugated microporous polymers: design, synthesis and application, Chem. Soc. Rev., 42 (2013), pp.8012–8031.
5. Y. Zhang, S. N. Riduan, Functional porous organic polymers for heterogeneous catalysis, Chem. Soc. Rev., 41 (2012), pp.2083–2094.
6. X. Feng, X. Ding, D. Jiang, Covalent organic frameworks, Chem. Soc. Rev., 41 (2012), pp.6010–6022.
7. N. Huang, P. Wang, D. Jiang, Covalent organic frameworks: a materials platform for structural and functional designs, Nat. Rev. Mater., 1 (2016), 16068.
8. K. Geng, T. He, R. Liu, K. T. Tan, Z. Li, S. Tao, Y. Gong, Q. Jiang, and D. Jiang, Covalent organic frameworks: design, synthesis, and functions. Chem. Rev. doi.org/10.1021/acs.chemrev.9b00550.
9. T. Ben, H. Ren, S. Ma, D. Cao, J. Lan, X. Jing, W. Wang, J. Xu, F. Deng, J. M. Simmons, S. Qiu and G. Zhu, Targeted synthesis of a porous aromatic framework with high stability and exceptionally high surface area, Angew. Chem. Int. Ed., 48 (2019), pp.9457–9460.

10. L. Tan and B. Tan, Hypercrosslinked porous polymer materials: design, synthesis, and applications, Chem. Soc. Rev., 46, (2017), pp.3322–3356.

11. S. Yao, X. Yang, Miao Yu, Y. Zhang, J. Jiang, High surface area hypercrosslinked microporous organic polymer networks based on tetraphenylethylene for CO_2 capture, J. Mater. Chem. A, 2 (2014) pp.8054–8059.

12. J. Huang, X. Zhou, A. Lamprou, F. Maya, F. Svec, S. R. Turner, Nanoporous polymers from cross-linked polymer precursors via tert-butyl group deprotection and their carbon dioxide capture properties, Chem. Mater., 21 (2015), pp.7388–7394.

13. Q. Chen, M. Luo, P. Hammershoj, D. Zhou, Y. Han, B. Laursen, C. Yan, B. Han, J. Am. Chem. Soc., 134 (2012), pp.6084–6087.

14. X. Zhu, C. Tian, G. M. Veith, C. W. Abney, J. Dehaudt, S. Dai, In situ doping strategy for the preparation of conjugated triazine frameworks displaying efficient CO_2 capture performance, J. Am. Chem. Soc., 138 (2016), pp.11497–11500.

15. M. Janeta, W. Bury and S. Szafert. Porous silsesquioxane–imine frameworks as highly efficient adsorbents for cooperative iodine capture. ACS Applied Mater. Interfaces, 10 (2018), pp.19964–19973.

16. T. Geng, C. Zhang, M. Liu, C, Hu, G, Chen. Preparation of biimidazole-based porous organic polymers for ultrahigh iodine capture and formation of liquid complexes with iodide/polyiodide ions. J. Mater. Chem. A 8 (2018), pp. 2820–2826.

17. S. J. Yang, X. Ding, B. H. Han, Conjugated microporous polymers with extended π-structures for organic vapor adsorption, Macromolecules, 3 (2018), pp.947–953.

18. Y. Yuan, P. Cui, Y. Tian, X. Zou, Y. Zhou, F. Sun, G. Zhu, Coupling fullerene into porous aromatic frameworks for gas selective sorption, Chem. Sci., 7 (2016), pp.3751–3756.

19. Z. Li, X. Feng, Y. Zou, Y. Zhang, H. Xia, X. Liu, Y. Mu, A 2D azine-linked covalent organic framework for gas storage applications, Chem. Commun., 50 (2014), pp.13825–13828.

20. Z. Li, Y. Zhi, X. Feng, X. Ding, Y. Zou, X. Liu, Y. Mu, An Azine-linked covalent organic framework: synthesis, characterization and efficient gas storage, Chem. Eur. J., 21 (2015), pp.12079–12084.

21. N. Huang, P. Wang, M. A. Addicoat, T. Heine, D. Jiang, Ionic covalent organic frameworks: design of a charged interface aligned on 1D channel walls and its unusual electrostatic functions, Angew. Chem. Int. Ed., 56 (2017), pp.4982–4986.

22. Janeta, M.; Bury, W.; Szafert, S. Porous silsesquioxane–imine frameworks as highly efficient adsorbents for cooperative iodine capture. ACS Appl. Mater. Interfaces 10 (2018), 23.

23. H. Gao, L. Ding, H. Bai, A. Liu, S. Li, L. Li, Pitch-based hyper-cross-linked polymers with high performance for gas adsorption, J. Mater. Chem. A, 4 (2016), pp.16490–16498.

24. N. Song, H. Yao, T. Ma, T. Wang, K. Shi, Y. Tian, Y. Zou, S. Zhu, Y. Zhang, S. Guan, Fabrication of microporous polyimide networks with tunable pore size and high CO_2 selectivity, Chem. Eng. J., 368 (2019) pp. 618–626.

25. K. Shia, N. Song, Y. Zou, S. Zhua, H. Tan, Y. Tian, B. Zhang, H. Yao, S. Guan, Porphyrin-based porous polyimides: Synthesis, porous structure, carbon dioxide adsorption, Polymer, 169 (2019), pp. 160–166.

26. Z. Li, H. Li, H. Xia, X. Ding, X. Luo, X. Liu, Y. Mu, Triarylboron-linked conjugated microporous polymers: sensing and removal of fluoride Ions, Chem. Eur. J., 21 (2015), pp.17355–17362.

27. Z. Li, Y. Zhang, H. Xia, Y. Mu, X. Liu, A robust and luminescent covalent organic framework as a highly sensitive and selective sensor for the detection of Cu^{2+} ions, Chem. Commun., 52 (2016), pp. 6613–6616.

28. Z. Li, N. Huang, K. H. Lee, Y. Feng, S. Tao, Q. Jiang, Y. Nagao, S. Irle, D. Jiang, Light-emitting covalent organic frameworks: fluorescence improving via pinpoint surgery and selective switch-on sensing of Anions, J. Am. Chem. Soc., 39 (2018) pp.12374–12377.

29. L. Guo, M. Wang, X. Zeng and D. Cao, Luminescent porous organic polymer nanotubes for highly selective sensing of H_2S, Mater. Chem. Front., 1 (2017), pp. 2643–2650.

30. E. Merino, E. Verde-Sesto, E. M. Maya, M. Iglesias, F. Sánchez and A. Corma, Synthesis of structured porous polymers with acid and basic sites and their catalytic application in cascade-type reactions, Chem. Mater., 25 (2013), pp.981–988.

31. M. Liu, L. Guo, S. Jin, B. Tan, Covalent triazine frameworks: synthesis and applications, J. Mater. Chem. A, 7 (2019), pp.5153-5172.

32. W. Xie, Di Cui, S. Zhang, Y. Xu, D. Jiang, Iodine capture in porous organic polymers and metal–organic frameworks materials, Mater. Horiz., 2019, Doi 10.1039/C8MH01656A.

33. P. Wang, Qing, Xu, Z. Li, W. Jiang, Q. Jiang, D. Jiang, Exceptional Iodine Capture in 2D Covalent Organic Frameworks, Adv. Mater., 30 (2018), 180199.

34. Z. Yin, Q. Xu, T. G. Zhan, Q. Y. Qi, Z. Wu and X. Zhao, Ultrahigh volatile iodine uptake by hollow microspheres formed from a heteropore covalent organic framework, Chem. Commun., 53 (2017), pp.7266–7269.

35. S. Xiong, X. Tang, C. Pan, L. Li, J. Tang, G. Yu, Carbazole-bearing porous organic polymers with a mulberry-like morphology for efficient iodine capture, ACS Appl. Mater. Interfaces, 11 (2019), pp.27335–27342.

36. M. Janeta, W. Bury, S. Szafert, Porous silsesquioxane–imine frameworks as highly efficient adsorbents for cooperative iodine capture, ACS Appl. Mater. Interfaces, 23 (2018), pp.19964–19973.

37. D. Xu, J. Guo, F. Yan, Porous ionic polymers: design, synthesis, and applications, Prog. Poly. Sci., 79 (2018), pp.121–143.

38. Y. Su, Y. Wang, X. Li, X. Li, R. Wang, Imidazolium-based porous organic polymers: anion exchange-driven capture and luminescent probe of $Cr_2O_7^{2-}$, ACS Appl. Mater. Interfaces, 29 (2016), pp.18904-18911.

39. J. Song, Y. Li, P. Cao, X. Jing, M. Faheem, Y. Matsuo, Y. Zhu, Y. Tian, X. Wang, G. Zhu, Synergic catalysts of polyoxometalate@cationic porous aromatic

frameworks: reciprocal modulation of both capture and conversion materials, Adv. Mater., 31 (2019), 1902444.

40. X. Shen, S. Ma, H. Xia, Z. Shi, Y. Mu, X. Liu, cationic porous organic polymers as an excellent platform for highly efficient removal of pollutants from water, J. Mater. Chem. A, 6 (2018), pp.20653–20658.

41. S. Hao, Y. Liu, C. Shang, Z. Liang, J. Yu, CO_2 adsorption and catalytic application of imidazole ionic liquid functionalized porous organic polymers, Polym. Chem., 8 (2017), pp.1833–1839.

42. Y. Liu, Y. Cui, C. Zhang, J. Du, S. Wang, Y. Bai, Z. Liang, X. Song, Post-cationic modification of a pyrimidine-based conjugated microporous polymer for enhancing the removal performance of anionic dyes in water, Chem. Eur. J., 24 (2018), pp.7480–7488.

43. Y. Hu, N. Dunlap, S. Wan, S. Lu, S. Huang, I. Sellinger, M. Ortiz, Y. Jin, S. Lee, W. Zhang, crystalline lithium imidazolate covalent organic frameworks with high Li-ion conductivity, J. Am. Chem. Soc., 18 (2019), pp.7518–7525.

44. Z. Yan, Y. Yuan, Y. Tian, D. Zhang, G. Zhu, Highly efficient enrichment of volatile iodine by charged porous aromatic frameworks with three sorption sites, Angew. Chem. Int. Ed., 54 (2015), pp.12733–12737.

45. G. Das, T. Prakasam, S. Nuryyeva, D. S. Han, A. Abdel-Wahab, J. Olsen, K. Polychronopoulou, C. Platas-Iglesias, Florent Ravaux, M. Jouiadf, Ali Trabolsi, Multifunctional redox-tuned viologen-based covalent organic polymers, J. Mater. Chem. A, 4 (2016), pp.15361–15369.

46. D. Shetty, J. Raya, D. S. Han, Z. Asfari, J. Olsen, A. Trabolsi, Lithiated polycalix[4]arenes for efficient adsorption of iodine from solution and vapor phases, Chem. Mater., 29 (2017), pp.8968–8972.

47. K. Jie, H. Chen, P. Zhang, W. Guo, M. Li, Z. Yang, S. Dai, A benzoquinone-derived porous hydrophenazine framework for efficient and reversible iodine capture, Chem. Commun., 54 (2018), pp.12706–12709.

48. Xu, Y. Zhu, W. Xie, S. Zhang, C. Yao, Y. Xu, Porous cationic covalent triazine-based frameworks as platforms for efficient CO_2 and iodine capture, Chem. Asian J., 14 (2019), pp.3259–3263.

49. S. A, Y. Zhang, Z. Li, H. Xia, M. Xue, X. Liu and Y. Mu, Highly efficient and reversible iodine capture using a metalloporphyrin-based conjugated microporous polymer, Chem. Commun., 50 (2014), pp.8495–8498.

50. H. Li, X. S. Ding, B. H. Han, Porous azo-bridged porphyrin–phthalocyanine network with high iodine capture capability, Chem. Eur. J., 22 (2016), pp.11863–11868.

51. Y. Li, W. Chen, W. Hao, Y. Li, L. Chen, Covalent organic frameworks constructed from flexible building blocks with high adsorption capacity for pollutants, ACS Appl. Nano Mater., 19 (2018), pp.4756–4761.

52. T. Geng, S. Ye, Z. Zhu, W. Zhang, Triazine-based conjugated microporous polymers with N,N,N′,N′-tetraphenyl-1,4-phenylenediamine, 1,3,5-tris(diphenylamino)benzene and 1,3,5-tris[(3-methylphenyl)-phenylamino]benzene

as the core for high iodine capture and fluorescence sensing of o-nitrophenol, J. Mater. Chem. A, 6 (2018), pp.2808–2816.

53. C. Yao, G. Li, J. Wang, Y. Xu and L. Chang, Template-free synthesis of porous carbon from triazine based polymers and their use in iodine adsorption and CO_2 capture, Sci. Rep., 8 (2018), 1867.

54. Y. H. Abdelmoaty, T. Tessema, Fatema Akthar Choudhury, O. M. El-Kadri,H. M. El-Kaderi, Nitrogen-rich porous polymers for carbon dioxide and iodine sequestration for environmental remediation, ACS Appl. Mater. Interfaces, 10 (2018), pp.16049–16058.

55. S. Xiong, J. Tao, Y. Wang, J. Tang, C. Liu, Q. Liu, Y. Wang, G. Yu, C. Pan, Uniform poly(phosphazene–triazine) porous microspheres for highly efficient iodine removal, Chem. Commun., 54 (2018), pp.8450–8453.

56. F. Ren, Z. Zhu, X. Qian, W. Liang, P. Mu, H. Sun, J. Liu, A. Li, Novel thiophene-bearing conjugated microporous polymer honeycomb-like porous spheres with ultrahigh iodine uptake, Chem. Commun., 52 (2016), pp.9797-9800.

57. X. Qian, Z. Q. Zhu, H. X. Sun, F. Ren, P. Mu, W. Liang, L. Chen, A. Li, Capture and reversible storage of volatile iodine by novel conjugated microporous polymers containing thiophene units, ACS Appl. Mater. Interfaces, 8 (2016), pp.21063–21069.

58. Y. Chen, H. Sun, R. Yang, T. Wang, C. Pei, Z. Xiang, Z. Zhu, W. Liang, A. Li, W. Deng, Synthesis of conjugated microporous polymer nanotubes with large surface areas as absorbents for iodine and CO_2 uptake, J. Mater. Chem. A, 3 (2015), pp.87-91.

59. D. Chen, Y. Fu, W. Yu, G. Yu, C. Pan, Versatile adamantane-based porous polymers with enhanced microporosity for efficient CO_2 capture and iodine removal, Chem. Eng. J., 334 (2018), pp.900–906.

60. H. Sun, P. La, R. Yang, Z. Zhu, W. Liang, B. Yang, A. Lia, W. Deng, Innovative nanoporous carbons with ultrahigh uptakes for capture and reversible storage of CO_2 and volatile iodine, J. Hazard. Mater., 321 (2017), pp.210–217.

61. H. Ma, J. J. Chen, L. Tan, J. H. Bu, Y. Zhu, B. Tan, C. Zhang, Nitrogen-rich triptycene-based porous polymer for gas storage and iodine enrichment, ACS Macro Lett., 5 (2016), pp.1039–1043.

62. J. Wang, K. Ai, L. Lu, Flame-retardant porous hexagonal boron nitride for safe and effective radioactive iodine capture, J. Mater. Chem. A, 7 (2019), pp.16850–16858.

63. X. He, S. Zhang, X. Tang, S. Xiong, C. Ai, D. Chen, J. Tang, C. Pan, G. Yu, Exploration of 1D channels in stable and high-surface-area covalent triazine polymers for effective iodine removal, Chem. Eng. J., 371 (2019), pp.314–318.

64. Y. Zhu, Y. J. Ji, D. G. Wang, Y. Zhang, H. Tang, X. R. Jia, M. Song, G. Yu, G. C. Kuang, BODIPY-based conjugated porous polymers for highly efficient volatile iodine capture, J. Mater. Chem. A, 5 (2017), pp.6622-6629.

65. C. Wang, Y. Wang, R. Ge, X. Song, X. Xing, Q. Jiang, H. Lu, C. Hao, X. Guo, Y. Gao, Donglin Jiang, A 3D covalent organic framework with exceptionally high iodine capture capability, Chem. Eur. J., 24 (2018), pp.585–589.

66. T. Geng, Z. Zhu, W. Zhang, Y. Wang, A nitrogen-rich fluorescent conjugated microporous polymer with triazine and triphenylamine units for high iodine capture

and nitro aromatic compound detection, J. Mater. Chem. A, 5 (2017), pp.7612–7617.